

# The influence of branch length on the deformation and microstructure of polyethylene

R. A. Bubeck and H. M. Baker

The Dow Chemical Company, Building 433A, Midland, MI 48640, USA

(Received 7 December 1981; revised 8 March 1982)

The length and number of side chain branches have a profound influence on the microstructure and physical properties of polyethylene (PE). For a series of linear PE copolymers: environmental stress cracking resistance (ESCR), melting points, creep resistance and modulus, and equilibrium spherulite size were all found to increase with increasing branch length (methyl to hexyl) at a given density and molecular weight. It is proposed that (at a fixed molecular weight) branch length and branch concentration determine spherulite size and, consequently, spherulitic boundary areas, in which the dry crazing/voiding occurs during the incubation period of environmental stress cracking (ESC). At a fixed density, decreased spherulite size contributes to greater spherulite boundary slip and increased creep at low (less than 2 MPa) stresses.

**Keywords** Branching; creep; deformation; environmental stress cracking resistance; microstructure; polyethylene

## INTRODUCTION

The environmental stress cracking process in polyethylene (PE) has been demonstrated to be a two-stage process involving an incubation time  $t_d$  and the actual crack growth<sup>1-3</sup>. The incubation time  $t_d$  increases with decreasing stress and appears to be the time necessary to form sufficient dry voiding/crazing ahead of a flaw when under stress and in contact with an aggressive environment that enhances the crazing/cracking process. A dry craze tip is the precursor to the environmental craze/crack and its growth velocity is liquid transport controlled, where capillary pressure is the driving force<sup>2</sup> in a fashion similar to the environmental crazing in glassy polymers<sup>4</sup> and in rubber-modified polystyrene<sup>5</sup>. The microstructure, as controlled by branching and the thermal history, can be expected to have a considerable influence on craze nucleation and growth during the environmental stress cracking (ESC) process in PE, as well as other physical properties. The purpose of this paper is to discuss the influence of branching on the microstructure of PE and,

consequently, on the kinetics of ESC in PE, the physics of which was established in a previous paper<sup>2</sup>. Effects of branching on creep at low applied stresses will be touched upon, also.

## EXPERIMENTAL

The resins studied include a 4.0 to 5.0 melt index (*MI*) series of linear polyethylene copolymers of ethylene with 1-propylene and 1-octene. These copolymers and a homopolymer comprise a density ( $\rho$ ) range of 0.964 g/cc to 0.919 g/cc as listed in *Table 1*. A 25 *MI*,  $\rho = 0.920$  g/cc series of linear low density PE (LLDPE) copolymers of ethylene with 1-propylene, 1-butene, 1-hexene and 1-octene (as well as selected terpolymers) are listed in *Table 2*. Also included in *Table 2* is a conventional long chain branched low density polyethylene (LDPE). The linear polyethylenes were made by a low pressure process and the long chain branched LDPE was made by a high pressure process, both of which are briefly described by

*Table 1* PE branch-property listing (4.0–5.0 *MI* series)

Resin	Comonomer	$\rho$ (g/cc)	<i>MI</i>	<sup>1</sup> $T_m$ (°C)	<sup>2</sup> ESCR (s)	Spherulite size $\mu\text{m}$	$t_d$ (s)
A	None	0.964	5.0	136	40 000	10	10 000
B	P	0.954	4.0	134	80 000	20	28 000
C	P	0.935	5.0	129	13 000	15/6 <sup>3</sup>	4000
D	O	0.955	4.4	135	80 000	10	29 000
E	O	0.935	4.0	132	110 000	49	35 000
F	O	0.935	4.5	132	120 000	40	36 000
G	O	0.919	5.0	128	130 000	65	40 000

<sup>1</sup>Primary crystalline melting endotherm (d.s.c.)

<sup>2</sup>ESCR at  $K_I = 0.2$  MPa m<sup>1/2</sup> at  $T = 50^\circ\text{C}$  in 10% CO–630

<sup>3</sup>#/# segregated spherulites – bimodal size distribution

$t_d$  = incubation time for ESC by time lapse photography

O = Octene (hexyl branch)

P = Propylene (methyl branch)

Table 2 PE branch-physical property relationships (25 MI, fixed  $\rho \approx 0.920$  g/cc series)

Resin	Weight % of branching <sup>1</sup>	$T_m$ (°C)	Average spherulites size ( $\mu\text{m}$ )	ESCR <sup>2</sup> (s)	Creep modulus <sup>3</sup>	% Creep strain <sup>4</sup> 1000 (h)
H	O	128	82	58 000	214 MPa	2.0
I	60% H/40% O	128	48	38 000	—	—
J	40% B/60% O	128	36	19 000	—	—
K	B	127	30	10 000	200 MPa	2.4
L	45% P/55% O	120	27	6000	173 MPa	2.6
M	P	118	18/10	4000	159 MPa	2.9
N	HOMO	112	9	1200	145 MPa	3.1

<sup>1</sup> O = Octene (hexyl branch)

H = Hexene (butyl branch)

B = Butene (ethyl branch)

P = Propylene (methyl branch)

HOMO = Homopolymer — long chain branching

<sup>2</sup> ESCR,  $K_I = 0.1$  MPa  $\text{m}^{1/2}$ , 50°C in 10% CO-630

<sup>3</sup> Creep modulus (ASTM Std. at 0.1 h)

<sup>4</sup> Applied stress = 1.725 MPa



Figure 1 Generalized diagram of linear polyethylene molecular structure

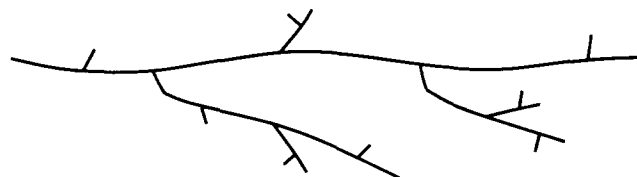


Figure 2 Generalized diagram of long chain branched low density polyethylene homopolymer

Cook and Lepper<sup>6</sup>. Schematics of the linear and long chain branched PE molecular structures are shown, respectively in Figures 1 and 2.

All samples for mechanical testing or microstructural examination were compression moulded except for the one blow moulded case noted later in the discussion. Because the compression moulding conditions have considerable influence on the equilibrium spherulite sizes reported here, the moulding procedure is described as follows. Compression moulded PE samples were fabricated from 15.25 cm  $\times$  15.25 cm compression moulded plaques 1.8 mm thick. Sufficient resin was placed in a mould sandwiched between two chrome-plated steel sheets in a heated press. The sheets were lubricated with 'a touch' of fluorogluid mould release agent. The PE was first heated at 171°C in the mould for 10 min. Platten force was then raised to 500 lbs and the temperature was allowed to decrease to 130°C. Platten force was then increased to 20 000 lbs and the temperature was allowed to fall to 104°C. Platten force was then increased to 40 000 lbs. When the temperature had fallen to 71°C, moderate water cooling in the hot press was carried out until the sample reached room temperature.

A blow moulding grade linear high density polyethylene (HDPE) resin ( $\rho = 0.954$  g/cc,  $MI = 0.25$ ) was also included to demonstrate the effect of processing on ESCR and morphology. ESC test samples were cut vertically from blow moulded bottle walls from bottles moulded in a Beckum blow moulding machine with the mould cooling water temperature set at 22°C.

The mechanical properties measured include environ-

mental stress crack resistance (ESCR) and constant load creep. ESCR was determined in a 10% Igepal CO-630 solution at 50°C by a double-edge-notch fracture mechanics method<sup>2,3</sup> measured as a function of the first stress intensity parameter  $K_I$ . Time lapse photography was performed for measuring crack growth. Tensile creep measurements were made at an applied stress of 1.725 MPa at 23°C and conform to ANSI/ASTM D2990-77<sup>7</sup>. Differential scanning calorimetry (d.s.c.) melting points were also determined using a heating rate of 5°C/min using a Dupont 990 d.s.c. unit.

Two electron microscopy specimen preparation techniques were used for microstructure examination. Transmission electron microscopy (TEM) observations were made on ultramicrotomed samples prepared by the Kanig<sup>8,9</sup> chlorosulphonic acid-uranyl acetate selective staining technique. This technique permits distinction between crystalline and amorphous regions. It also stabilizes the polyethylene for cold stage ultramicrotoming and against electron radiation. Such stabilization permits the preservation and observation of stable crazes and voiding that result from mechanical deformation. Figure 3 shows the dry craze tip of an environmental stress crack in a spherulite boundary region of sample F, as well as the crystalline lamellar structure. Scanning electron microscopy (SEM) was performed on chromic acid etched surfaces of polyethylene that were prepared by cold stage



Figure 3 Bright field transmission electron photomicrograph of a dry craze in a spherulite boundary region at the tip of an environmental stress crack in sample F. Marker = 0.33  $\mu\text{m}$

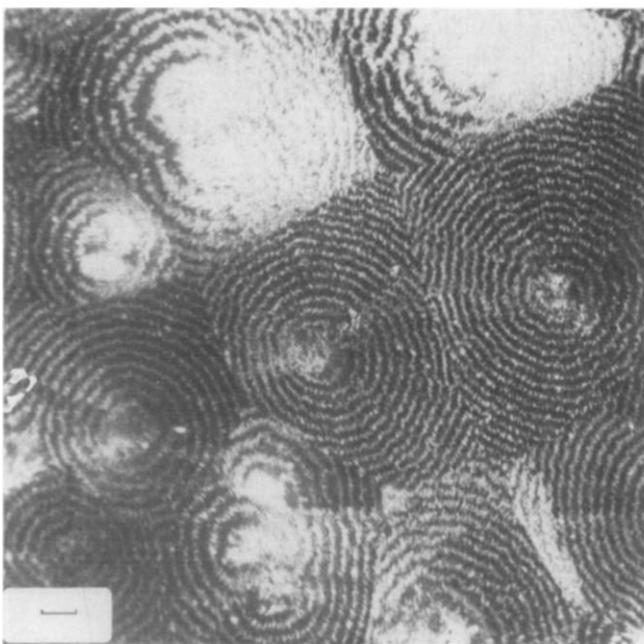


Figure 4 Scanning electron photomicrograph of spherulites in a linear low density ethylene-octene copolymer sample H. Marker = 7.2  $\mu\text{m}$

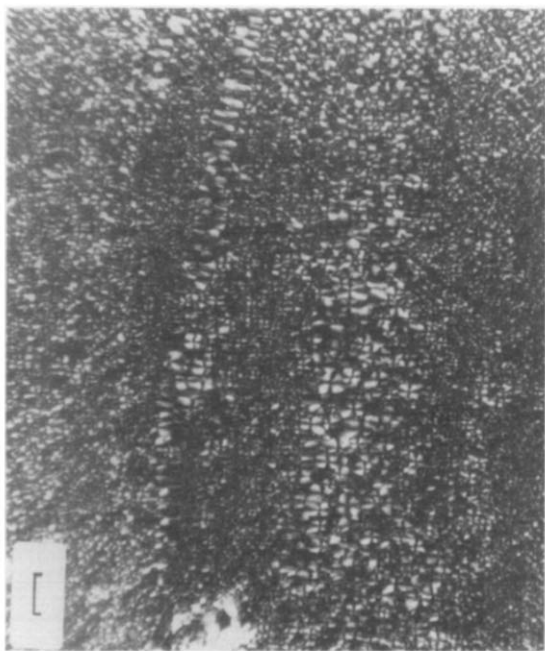


Figure 5 Light inference photomicrograph showing alternating layers of relatively large and small spherulites in compression moulded Sample C. 1 cm = 30  $\mu\text{m}$

ultramicrotoming. The SEM technique was used to measure spherulite size and observe spherulitic features such as boundaries and rings. Such a result is shown for a LLDPE ethylene-octene copolymer in Figure 4. In addition, some observations were made on selected microtomed samples by light interference microscopy.

## RESULTS AND DISCUSSION

Results for the 4.0–5.0 MI series of PE resins in Table 1 indicate that for the homopolymer and the 1-octene copolymer group that ESCR, the incubation time  $t_d$  for ESC, and average spherulite size all increase with decreasing density (increasing branching). The 1-propylene co-

polymers, starting from the homopolymer (A), were found to have maxima for ESCR,  $t_d$  for ESC, and average spherulite size at  $\rho = 0.954$  g/cc. Sample C at  $\rho = 0.935$  has a bimodal spherulite size (i.e., alternating layers of larger or smaller spherulites) and considerably reduced ESCR and  $t_d$ . Alternating layers of larger and smaller spherulites in sample C are shown in the light interference micrograph, of Figure 5. The results in Table 2 for the 25 MI, 0.920 g/cc series indicate that ESCR, average spherulite size, creep modulus, and the primary melting endotherm temperature all increase with increasing branch length for samples H through M. The creep strain at low applied stresses of less than 2 MPa decreases with increasing branch length.

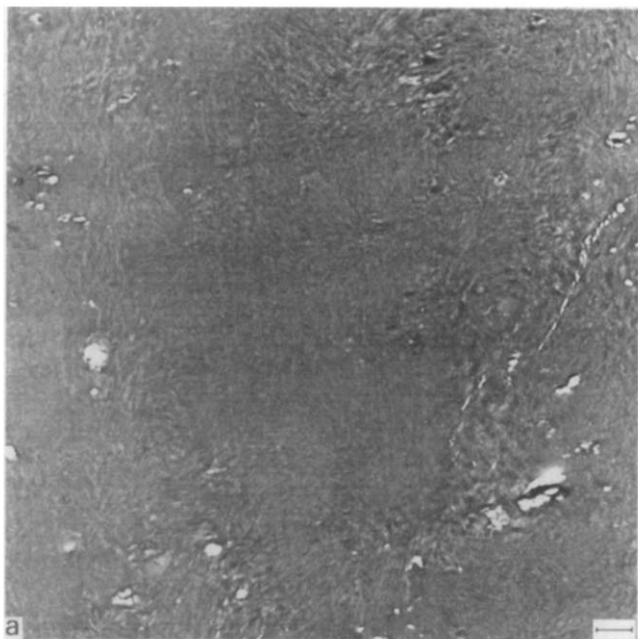
The average spherulite size increases with decreasing density (and increasing branch concentration) for the octene copolymer series in Table 1. Increasing the branch concentration results in decreasing the density of PE (see, for example, ref 11). A lower mole per cent concentration of branches is usually required of a longer branch-type to result in a given density. Apparently, a longer branch (in the methyl to hexyl branch length range) is more effective in suppressing crystallinity, and the resulting decrease in crystallite nucleation results in a larger average spherulite size for a longer branch.

The long chain branched LDPE sample N has the smallest average spherulite size, lowest melting point and poorest physical properties. Branches in linear PE copolymers have been shown to induce crystal unit cell distortion by Florin *et al.*<sup>10</sup>. The observation by Florin *et al.* and the mechanical property results presented here, in combination, suggest that when a branch is too long, it behaves as a main chain and that the secondary side branches attached to it primarily influence the resulting properties and microstructure. Thus, the branching in conventional LDPE homopolymers has a negative influence on the ESCR and the creep behaviour. The d.s.c. measurements in Table 3 show multiple melting endotherms  $T_m$  for the LLDPE resins, which indicates a heterogeneous branching distribution. The single  $T_m$  for the sample N LDPE indicates random branching.

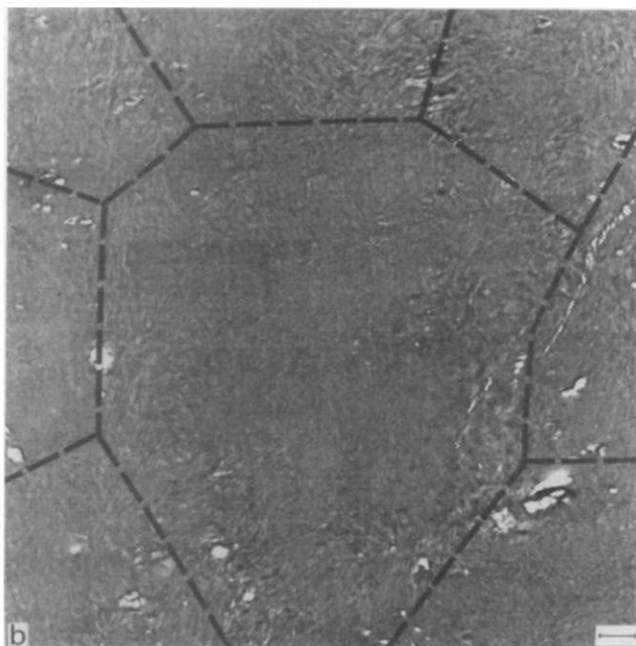
The incubation time is the important ESC difference between most polyethylenes rather than the actual crack growth rate and is associated with the dry voiding/crazing necessary to allow the ESC process to proceed. The TEM photomicrograph of Figure 6 (a and b) shows the area ahead of an environmental craze/crack in PE sample F. In this area the formation of microvoids occurs primarily in the disordered spherulite boundaries. Thus, a path of weakness is formed for the actual craze/crack to follow. The process for this proposed model is shown schematically in Figure 6. For a fixed molecular weight, decreasing the spherulite size provides more internal spherulitic surface area and, consequently, the ESC incubation time

Table 3 D.s.c. data for polyethylenes in Table 2

Resin	Weight % of branching	Primary endotherm $T_m$ ( $^{\circ}\text{C}$ )	Secondary endotherms ( $^{\circ}\text{C}$ )
H	100% O	128	120, 106
I	60% H/40% O	128	122, 105
J	40% B/60% O	128	119, 107
K	100% B	127	121, 106
L	45% P/55% O	120	125, 106
M	100% P	118	124, 102
N	HOMO	112	—



**Figure 6a** Bright field transmission electron photomicrograph of intermediate density polyethylene sample F showing dry voiding occurring primarily in spherulite boundaries in the area head of an environmental stress crack. The crack is approaching from the right side of the micrograph. Marker = 3.5  $\mu\text{m}$



**Figure 6b** Same as *Figure 6a*, but with the position of the spherulite boundaries approximately indicated with broken lines

and ESCR decrease. This observation provides an explanation for why ESCR can increase with decreasing density (such as in the cases of Sample A and Samples D through G in *Table 1*), even though the yield strength decreases with decreasing density. In addition, at a fixed density and molecular weight, the creep data for the samples listed in *Table 2* indicate, that at low stresses, a smaller spherulite size enhances overall spherulite boundary slip that can contribute to increased creep.

A special case of the dry voiding/crazing process ahead of a crack occurs with intermediate density PE (IMDPE) Sample C. Elston has shown that both the density and the

melting point increase as the branching distribution becomes more heterogeneous for a given side branch concentration<sup>11</sup>. If the branching is sufficiently heterogeneous in portions of the PE and the branch concentration is very high, for example in the IMDPE and LLDPE 1-propylene copolymers, then it is believed that alternating layers composed of spherulites of distinctly different sizes and density result. Dry crazing and delamination can occur between the layers of very different lamellar morphology at the spherulite layer boundaries, as shown in *Figure 8*, and, consequently, a greatly reduced  $t_d$  and ESCR result. Sample C exhibits two d.s.c. melting endotherms: a primary one at 129°C and a secondary one at 125°C. The less prominent endotherm at 125°C corresponds to the PE specie of relatively lower density (which is the lesser of the two types of observable morphologies) shown on the right side of the photomicrograph in *Figure 9*. A similar case exists for the propylene copolymer sample M, which exhibits a secondary melting endotherm at 124°C. In this case the major morphological component is a lower relative density rather than a higher density.

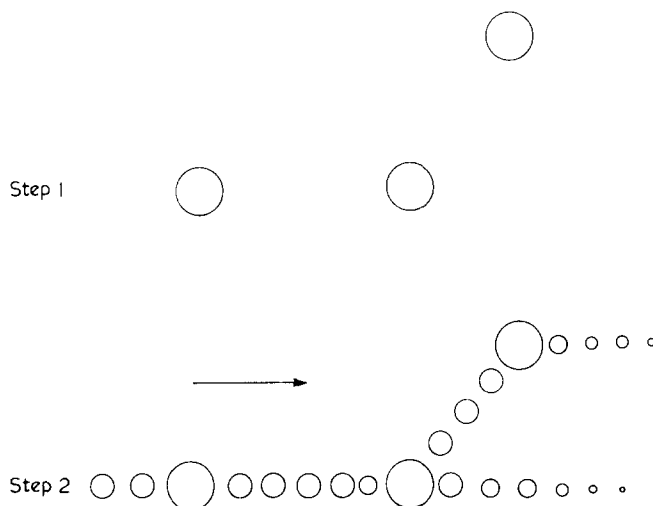


**Figure 7** Diagram of the two stage dry void/crazing process ahead of an environmental stress crack in polyethylene: Step 1, large microvoids ( $\sim 1 \mu\text{m}$  diameter) form preferentially at spherulite boundaries upon application of stress. Step 2, craze/crack grows following the line source of weakness formed by the large microvoids in the spherulite boundaries. Aggressive liquid flows down the craze, breaks down fibrils, and forms a crack

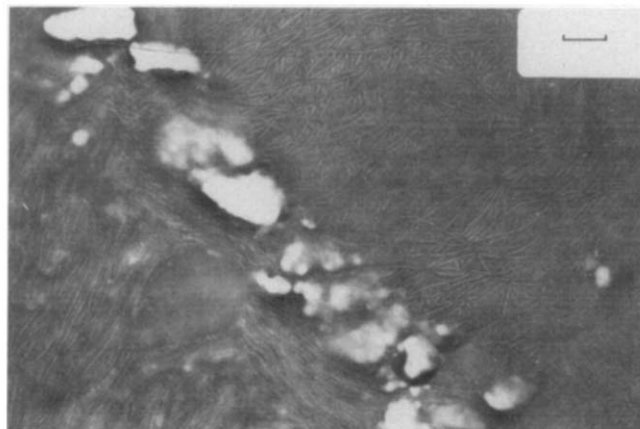


**Figure 8** Bright field transmission electron photomicrograph showing dry crazing between layers of relatively higher (left of craze) and lower (right of craze) densities in polyethylene sample C resulting in delamination and poor ESCR. Marker = 0.3  $\mu\text{m}$

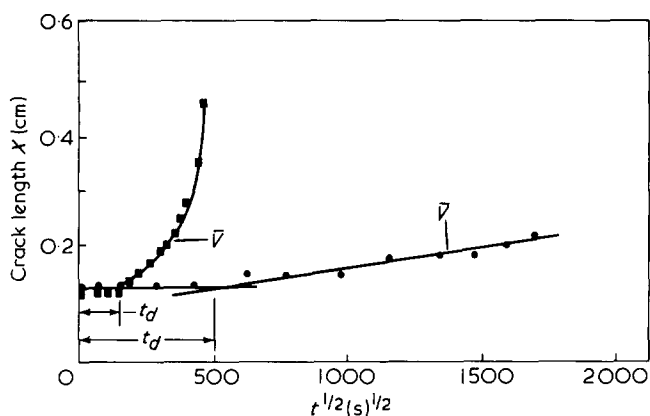


Figure 9 Time lapse photography data for crack length  $X$  versus root time  $t^{1/2}$  for HDPE ( $\rho = 0.954$  g/cc,  $MI = 0.25$ ) at  $K_I = 0.18$  MPa  $m^{1/2}$ ,  $T = 50^\circ\text{C}$  in 10% CO-630. Average spherulite sizes are  $0.5\ \mu\text{m}$  and  $2.5\ \mu\text{m}$ , respectively for the blow moulded (■) and compression moulded (●) conditions. The incubation times  $t_d$  and average crack growth velocities  $\bar{V}$  are  $t_d = 62\ 500$  s and  $\bar{V} \approx 1.5 \times 10^{-6}$  cm  $s^{-1}$  for the blow moulded condition, and  $t_d = 250\ 000$  s and  $\bar{V} = 3.5 \times 10^{-8}$  cm  $s^{-1}$  for the compression moulded condition

The time lapse photography data in Figure 9 for a HDPE ( $\rho = 0.954$  g/cc,  $MI = 0.25$ ) for environmental craze/crack growth for both the compression moulded and blow moulded samples agree with the proposed model. The blow moulded sample has both the smaller spherulite size and the lower  $t_d$  and ESCR. The average crack growth velocity  $\bar{V}$  is also greater for the blow moulded sample.

Three qualifications should be considered with the proposed model. One is that it certainly does not preclude *trans*-spherulitic craze/crack growth in bulk PE. What is proposed here is that the nucleation stage of craze formation is greatly favoured within the spherulite boundaries. The second is that increased molecular weight (i.e., decreased  $MI$ ) reduces the average spherulite size and increases the physical properties and this can be reconciled with the model. One must recognize that increasing molecular weight has been shown by Keith *et al.*<sup>12</sup> to also increase the number, length and width of the intercrystalline links that bridge the spherulite boundaries. This

condition outweighs the spherulite boundary area increase. Finally, different environments result in both different  $t_d$  and crack growth velocities. For example, isopropanol induces a  $t_d$  that is typically twice that measured in 10% Igepal. It is proposed that the aggressive liquid initially penetrates the PE under load a very short distance from the material surface, preferentially in spherulite boundaries. A craze soon results, the dry tip of which jumps forward from the immediate vicinity of the liquid (a strain energy release process) and triggers the general void/craze nucleation process described. The more aggressive the liquid is, the more the process in the spherulite boundaries ahead of the craze/crack is enhanced.

## ACKNOWLEDGEMENTS

Useful discussions on this material with F. J. McGarry of the Massachusetts Institute of Technology and E. J. Kramer of Cornell University are greatly appreciated.

## REFERENCES

- 1 Bubeck, R. A. *ACS Organic Coatings Plast. Chem. Preprints* 1979, **41**, 481
- 2 Bubeck, R. A. *Polymer* 1981, **22**, 682
- 3 Bandyopadhyay, S. and Brown, H. R. *J. Polym. Sci., Polym. Phys. Edn.* 1981, **19**, 749
- 4 Kramer, E. J. and Bubeck, R. A. *J. Polym. Sci., Polym. Phys. Edn.* 1978, **16**, 1195
- 5 Bubeck, R. A., Arends, C. B., Hall, E. L. and Vander Sande, J. B. *Polym. Eng. Sci.* 1981, **21**, 10, 624
- 6 Cook, J. A. and Lepper, S. E. *Soc. Plastics Engineers 38th Annual Technical Conference Technical Papers* 1980, **26**, 490
- 7 '1980 Annual Book of ASTM Standards, Plastics-General Test Methods; Nomenclature', (Part 35), 1980, 759, American Society for Testing and Materials, Philadelphia, Pa, USA
- 8 Kanig, G. *Kolloid-Z. Z. Polymere* 1973, **251**, 782
- 9 Kanig, G. *Kunststoffe* 1979, **64**, H9, 470
- 10 Florin, B., Spitz, R., Douillard, A., Guyot, A., Boyer, R. F., Denny, L. R. and Kumler, P. L. *Eur. Polym. J.* 1980, **16**, 1079
- 11 Elston, C. T. United States Patent No. 3,645,992, Feb. 29, 1972
- 12 Keith, H. D., Padden, Jr., F. J. and Vadimsky, R. G. *J. Polym. Sci. A-2* 1966, **4**, 267